LEGIBILITY NOTICE

A major purpose of the Technical Information Center is to provide the broadest dissemination possible of information contained in DOE's Research and Development Reports to business, industry, the academic community, and federal, state and local governments.

Although a small portion of this report is not reproducible, it is being made available to expedite the availability of information on the research discussed herein.

1

LA-UR -89-3600

CONF-8910121--1

Los Alamos National Laboratory is operated by the University of California for the United States Department of Energy under contract W-7405-ENG-36

LA-UR--89-3600

DE90 002409

TITLE: THE DESIGN AND PERFORMANCE OF THE FNAL HIGH-ENERGY POLARIZED BEAM FACILITY

AUTHOR(S): Nobuyuki Tanaka

SUBMITTED TO Manuscript of talk presented at the 1989 IUCF Topical Conference "Physics with Polarized Beams on Polarized Targets, MCCormick's Creek State Park, Spencer, Indiana, October 16-18, 1989

THE DESIGN AND PERFORMANCE OF THE FNAL HIGH-ENERGY POLARIZED BEAM FACILITY[a]

Nobuyuki Tanaka
(For the E-581/704 Collaboration[b])

Los Alamos National Laboratory
P. O. Box 1663, MS H841
Los Alamos, NM 87545

1. Introduction

We describe a new polarized-proton and -antiproton beam with 185-GeV/c momentum in the Fermilab MP beam line which is currently operational. The design uses the parity-nonconserving decay of lambda and antilambda hyperons to produce polarized protons and antiprotons, respectively. A beam-transport system minimizes depolarization effects and uses a set of 12 dipole magnets that rotate the beam-particle spin direction. A beam-tagging system determines the momentum and polarization of individual beam particles, allowing a selection of particles in definite intervals at momentum and polarization. We measured polarization of the beam by using two types of polarimeters, which verified the determination of polarization by a beam-particle tagging system. Two of these processes are the inverse-Primakoff effect[1] and the Coulomb-nuclear interference (CNI) in elastic proton-proton scattering.[2] Another experiment[3] measured the π^0 production asymmetry of large-x_F values; this process may now be used as an on-line beam polarimeter.

Since polarized beams and polarized proton targets became available for use in high-energy experiments, various measurements of the polarized phenomena have been made. The physics objectives for the Fermilab polarized beam facility up to 185 GeV/c are in part based on the fact that there are already several experimental indications[4] that spin effects are significant at high energy. They are: (a) measurements of π^0 production at high $p\perp (p\perp > 2.0$ GeV/c) in proton-proton collisions at CERN and in π^- proton collision at Serpukhov revealed sizable asymmetries at 24 GeV/c and 40 GeV/c, respectively. (b) Hyperons produced at large x_F inclusively off nuclei and hydrogen at CERN, Fermilab, and ISR were observed to have high polarizations. (c) Inelastic scattering of longitudinally polarized electrons on longitudinally polarized protons at SLAC yielded a large asymmetry, implying that proton helicity orientation is communicated to the constituent quarks. Thus, spin dependence in quark-quark collisions can be inferred from measurements of spin dependence in proton-proton collisions in appropriate kinematic regions. A number of theoretical models have been introduced to explain these polarization phenomena and predictions for future measurements have been made.

2. Polarized Beam Facility

During the last decade, construction of a high-energy (above 100 GeV/c) polarized beam has been attempted. In order to eliminate possible complications involving depolarization at high energies, polarized protons can be produced from decaying hyperons, lambdas or sigmas. The Fermilab polarized-beam facility was constructed and operated during the TeV-II fixed target period.

A polarized proton beam from Λ^0 decay at Fermilab was suggested by Overseth[5] in 1969 using the fact that the protons from lambda decay are polarized along their direction of motion in the lambda rest frame. This polarization has been measured by Cronin and Overseth[6] to determine the relative amounts of s- and p-waves in the decay. For unpolarized lambda, the polarization of the proton in the direction of the motion is 64%. It has been shown that we can select protons or antiprotons at various momenta which are decaying around $\theta_{c.m.} = 90°$ from lambdas or antilambdas, respectively.[7] Spin direction in the lambda center-of-mass (decay frame) is shown in Fig. 1. We note that spin direction is almost unchanged

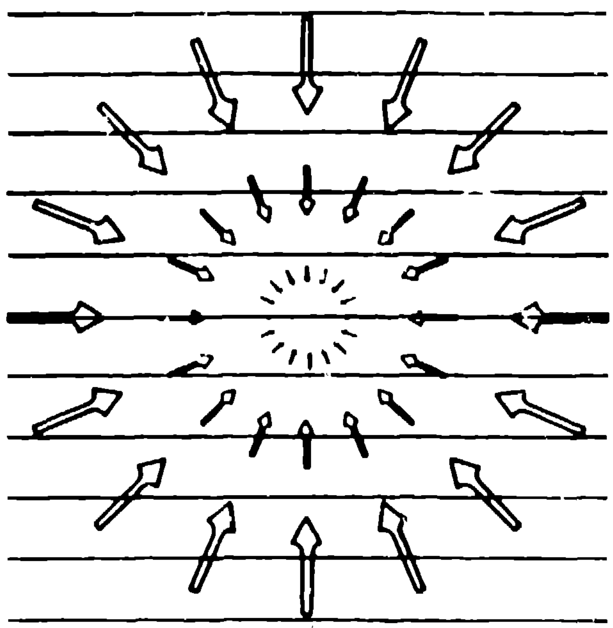

Fig. 1. Spin direction of protons vs decay angles. The spin direction is indicated by the arrow.

in transforming from the lambda-decay frame to the laboratory. Therefore protons and antiprotons decaying around $\theta_{c.m.} = 0°$ and 180° are longitudinally polarized while those with $\theta_{c.m.} = 90°$ are transversely polarized in the laboratory. Protons or antiprotons with $\theta_{c.m.} = 90°$ and $-90°$ have opposite laboratory decay angles, which are not zero. They can be distinguished from those decaying at $\theta_{c.m.} = 0°$ from lambda or antilambda with the production target as the source of the beam. Virtual sources for $|\theta_{c.m.}| = 90°$ particles are shown in Fig. 2.

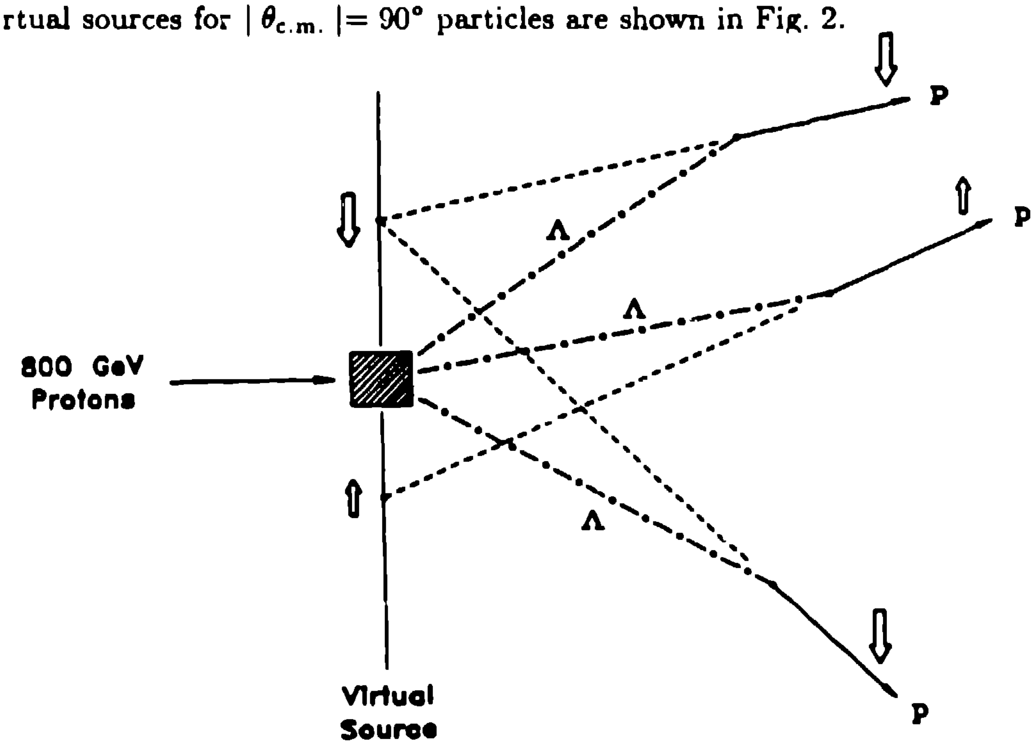

Fig. 2. Diagram of the primary production target, Λ decay process, and virtual source of polarized protons. Lambda particle, produced from incident 800-GeV/c protons on a beryllium target, decay into proton (shown) and pions (not shown). The polarization state of the proton is correlated with the position in the plane of the virtual source. The virtual source points are shown by the dashed lines traced back to this plane from the proton trajectory.

Unpolarized protons are accelerated to 800 GeV/c in the superconducting ring of the Tevatron and are extracted during a 20-sec spill. The extracted primary proton beam strikes a beryllium target and creates unpolarized lambdas. The primary beam line is shown in Fig. 3 where a parasitic target is typically used to produce an electron beam for calibration purposes. The secondary beam line up to 200 GeV/c is shown in Fig. 4. The Ŝ-type beam is produced before reaching the snake magnets which cause fast reversal of spin direction (typically every 10 spills). The snake magnets, consisting of 12 dipole magnets with 45° precessions, can also change the spin direction from $\hat{S}$ to $\hat{N}$ or $\hat{S}$ to $\hat{L}$ without altering beam direction and phase space before and after the magnets. These magnets are expected to control systematic errors by periodic reversal. A spin rotator is used in the beam line for two reasons: (a) to periodically reverse the polarization direction so that experimental systematic errors are controlled, and (b) to change the spin direction from horizontal ($\hat{S}$-spin direction), which is the spin component actually tagged, to vertical ($\hat{N}$ spin direction) or longitudinal ($\hat{L}$-spin direction) for different experimental measurements. Polarized protons from the virtual sources are focused in the tagging section, where both the momentum and polarization are selected.

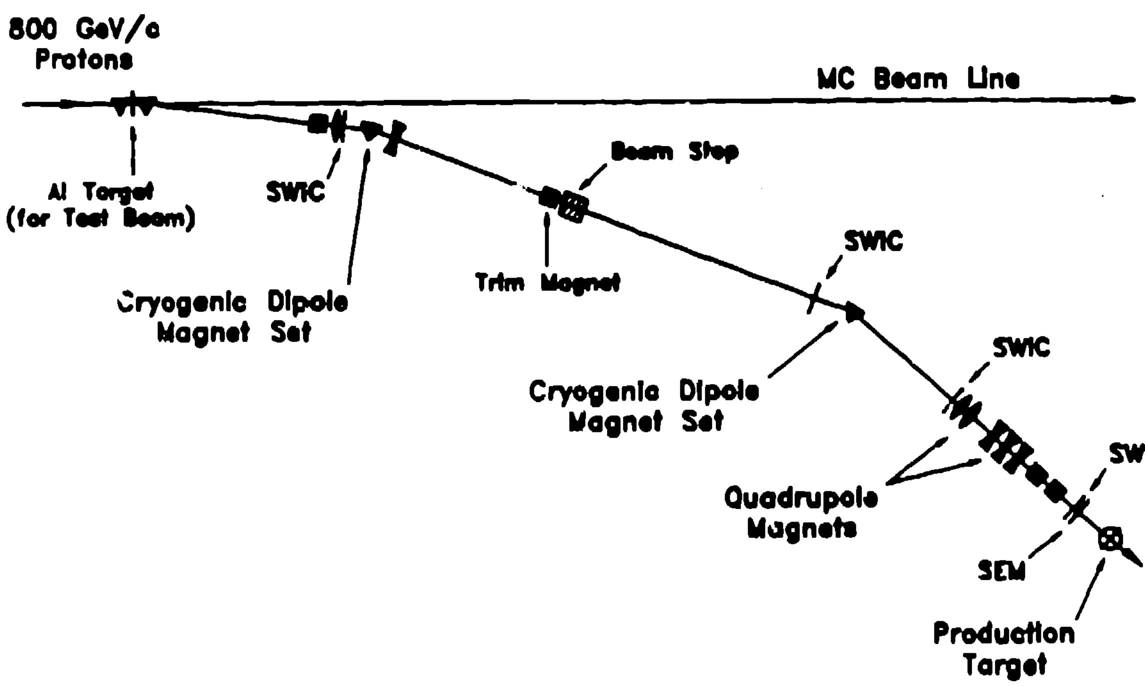

Fig. 3. Diagram of the MP primary beam line (not to scale). Shown are the split from the MC beam line, the two sets of cryogenic bending magnets, beam-line detectors (SWIC-segmented wire ion chambers and SEM-secondary emission monitor), and the production target.

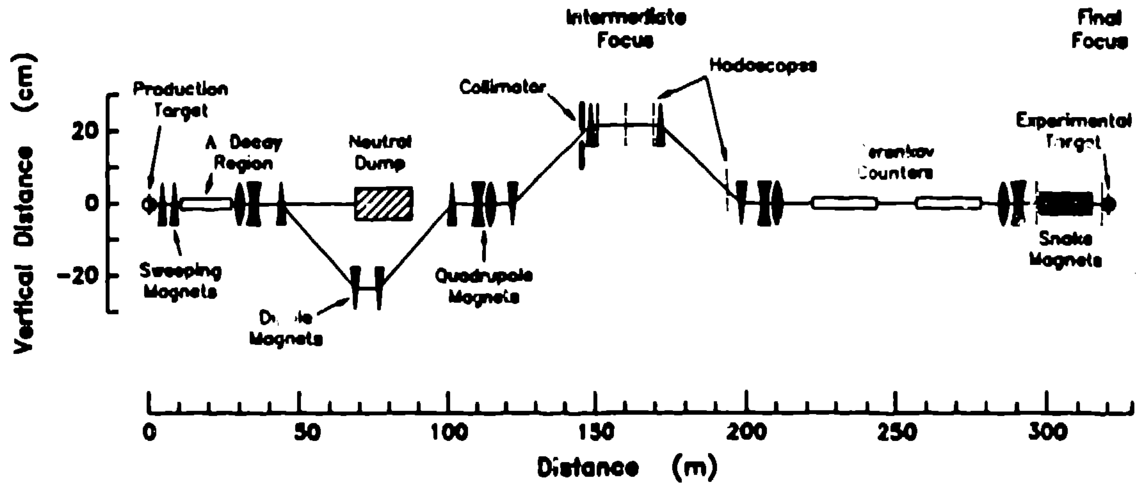

Fig. 4. Layout of elements along the MP polarized beam line. Shown here are a side view of the production target, neutral particle dump, adjustable collimator, beam tagging region, snake magnets, Cerenkov counters and experimental target. Note the difference in scale betweeen the horizontal and vertical axis.

Polarized protons have their polarization and momentum values electronically "tagged" within 250 ns after they reach the intermediate focus, using the correlation between the proton trajectory and its transverse polarization state. A total of ten beam scintillator hodoscopes, six located at the intermediate focus and four near the experimental target, detect the particle trajectory in the vertical (y) direction and the horizontal (x) direction. The beam is designed so that the particle momentum is measured in the vertical direction and the polarization in the horizontal. Polarized antiprotons are tagged in a similar manner as the polarized protons. The beam-tagging system must operate reliably and efficiently during data-taking periods. It is also used as an aid in optimizing the beam parameters and in beam tuning.

The polarization is strongly related to the x-position at the tagging section and the average polarization, $<P>$, and $I<P>^2$, where I represents actually measured beam intensity, is shown in Figs. 5 and 6, respectively, with respect to x in mm. The beam line was operated at 800 GeV/c incident momentum. The intensities of the total (not tagged) protons and antiprotons at 185 GeV/c were 1.5 × 10^7/spill and 7.5 × 10^5/spill, respectively, for incident protons with 10^{12}/spill. The intensities of tagged polarized protons and antiprotons with polarization higher than 35% were 8 × 10^6 and 4 × 10^5, respectively. The results are consistent with the tagged values.

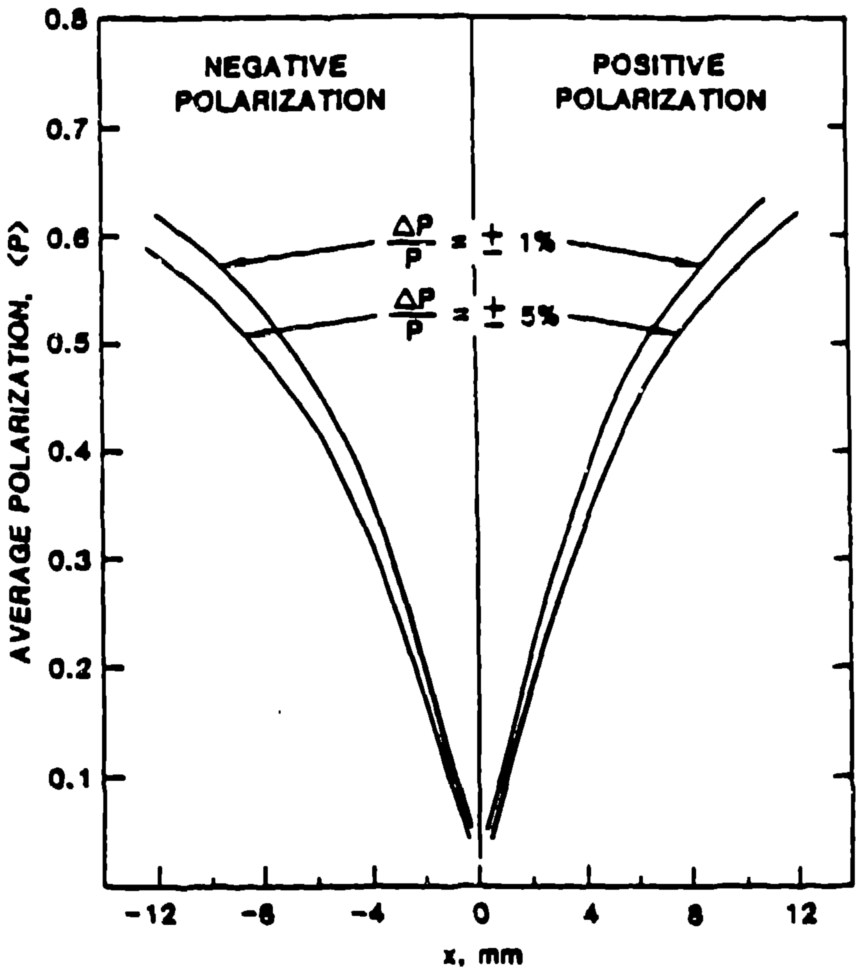

Fig. 5. <P> vs x in the tagging section.

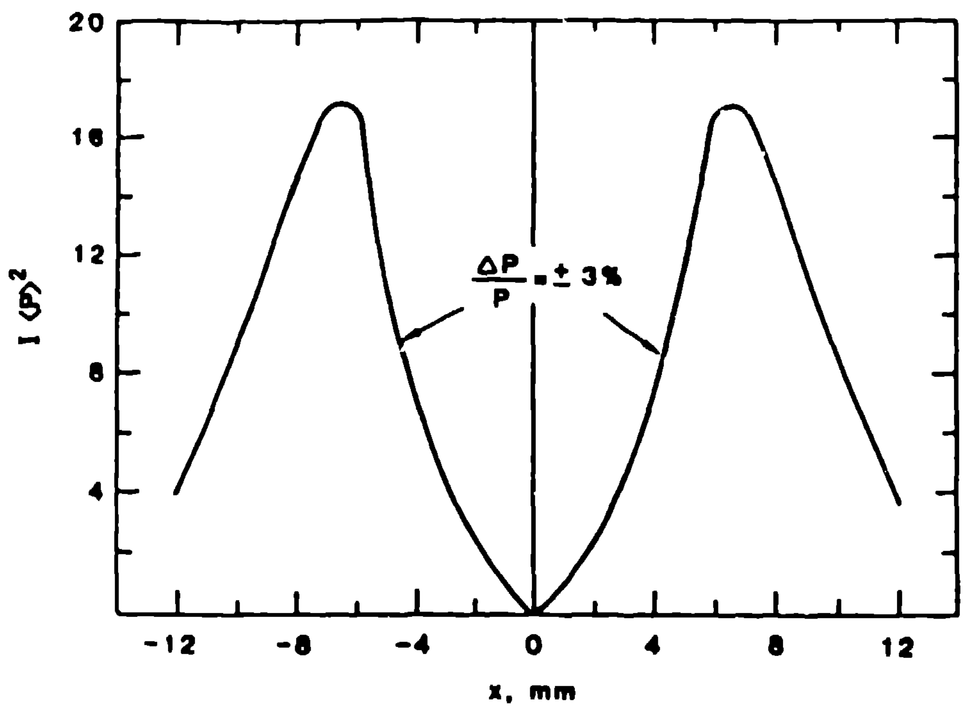

Fig. 6. I<P>^{2} (arbitrary unit) vs x in the tagging system.

3. Polarimeters

As discussed previously, the beam-tagging system assigns a polarization value for each beam particle relative to a known trajectory. An absolute measurement of the beam polarization is necessary to confirm these values. Two polarimeters have been developed for use with high-energy particles. The polarimeters are based on the following reactions that result in an asymmetry in the scattering process: (a) the dissociation of polarized protons in the Coulomb field of a nucleus (Primakoff-effect polarimeter), and (b) the Coulomb-nuclear interference in the elastic scattering of polarized protons by a proton target (CNI polarimeter). Because the analyzing power is known, the observed asymmetry measured by these polarimeters determines the absolute magnitude and sign of the polarization of the proton and antiproton beams. The measurement of the beam polarizations by these polarimeters serves both as a crucial test of the beam-tagging system and also as an independent measure of the beam polarization.

4. Primakoff-Effect Polarimeter

The Primakoff-effect polarimeter determines the proton-beam polarization by measuring the asymmetry of the Primakoff process, or coherent Coulomb dissociation.[1] An incident proton is converted to a p-π^0 system in the Coulomb field of a high-Z, nuclear target, given by

$$p + Z \rightarrow p + \gamma^* + Z \rightarrow p + \pi^0 + Z, \tag{1}$$

where Z is the high-Z nucleus and γ^* is the exchanged virtual photon. This reaction is related to low-energy photoproduction, including polarization effects, of a π^0 by a proton. The polarization of the 185-GeV/c proton beam can be determined from the measured value of the polarized-target asymmetry parameter from this low-energy ($\sim$ 700 MeV) photoproduction process.[8]

The cross section, $\sigma_{\rm Prim}$, of the Primakoff process is described in terms of the corresponding low-energy photoproduction cross section, $\sigma_{\rm photo}$, by:

$$\frac{d\sigma_{\rm Prim}}{dM_{{\rm p}\pi^0}\,dt\,d\phi} = \frac{\alpha Z}{\pi}\,\frac{\sigma_{\rm photo}}{M^2_{{\rm p}\pi^0} - M^2_{\rm p}}\,\frac{t'}{t^2}\,|F(t)|^2\,[1 + T(\theta)P_B\cos\phi]\,, \tag{2}$$

where $M_{{\rm p}\pi^0}$ is the invariant mass of the p-π^0 system, $M_{\rm p}$ is the proton mass, t is the four-momentum transfer squared and $t' = t - t_{\rm min} = -p_T^2$ for the virtual photon, $F(t)$ is the form factor for the target nucleus, $T(\theta)$ is the polarized-target asymmetry parameter from the photoproduction experiments, θ is the scattering angle between the π^0 and the virtual photon, P_B is the polarization of the incident protons, and ϕ is the azimuthal angle of the π^0 relative to the direction of the polarization vector of the incident proton.

The apparatus for the Primakoff-effect detector is shown in Fig. 7. It consists of a Pb target, 3-mm thick, surrounded by several lead-scintillator sandwich veto counters, a 156-element lead-glass calorimeter, 12 multiwire proportional chambers (MWPCs), a 2.6 T-m integrated-field analyzing magnet, and four trigger scintillation counters. A set of plastic scintillation counters placed upstream of the calorimeter is used as a charged-particle veto.

Five MWPCs, located upstream of the target, measure the trajectory of the incident beam particle. Downstream of the target, seven MWPCs trace the trajectory of the scattered proton and, along with the analyzing magnet, measure the proton momentum. Typical values measured for the proton momentum are from 110 to 160 GeV/c with a scattering angle from 1 to 4 mrad. The momentum resolution is about 1% (rms) and the angular resolution is about 6×10^{-2} mrad (rms), which includes the contribution of multiple scattering in the Pb target.

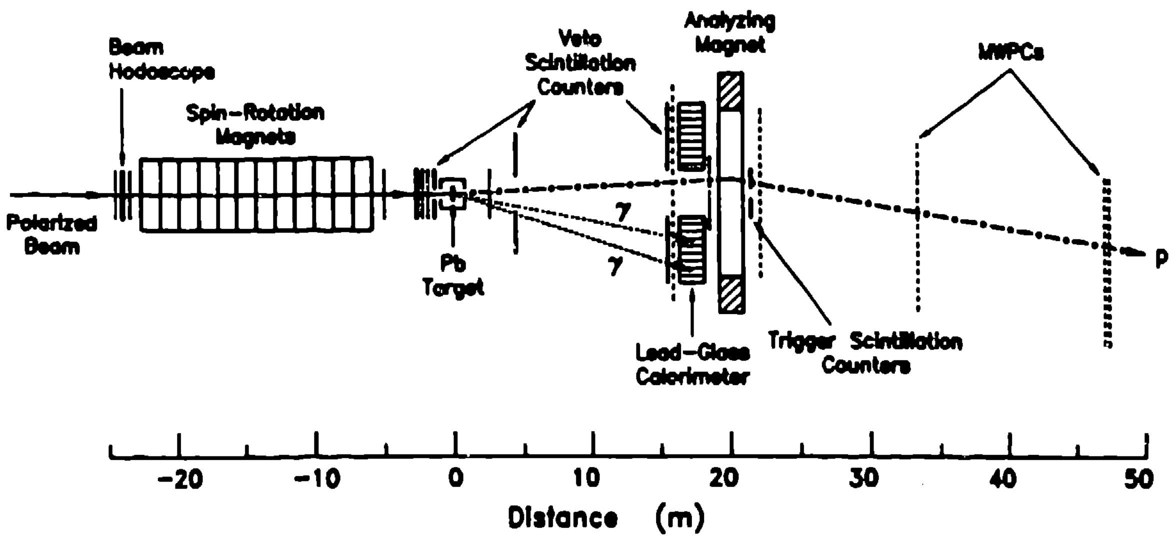

Fig. 7. Layout of the Primakoff-effect polarimeter. The dimensions transverse to the beam are not to scale.

The lead-glass calorimeter, located 17 m downstream of the target, detects the position and energy of the two photons from the π^0 decay. Each block of the 156-element array measures 3.8 cm × 3.8 cm × 45 cm, corresponding to about 19 interaction lengths, and is placed into an array. A hole in the center of the array, 4 × 4 blocks in size, allows passage through the calorimeter of the scattered protons and the unscattered beam. The typical energy range of the reconstructed π^0, as measured by the calorimeter, was from 30 to 70 GeV/c^2. The mass resolution for the reconstructed neutral pion was 8.4 MeV/c^2 (rms). The typical range of π^0 production angles was from 6 to 10 mrad, with a resolution of about 0.2 mrad (rms).

The detectors accept the events which are in the region of the maximum analyzing power $| t' | < 0.001$ (GeV/c)^2 $1.34 \leq M_{p\pi^0} \leq 1.50$ GeV/c^2, $70° \leq \theta^{\pi}_{c.m.} \leq 120°$ and $\Delta\phi = \pm 30°$ on both sides of the beam line.

The Primakoff-effect polarimeter collected data during about 50 hours, using a vertically-polarized proton beam at a rate of 10^7 incident protons per 20-sec spill on the Pb target. This produced a trigger rate of approximately 1000 events per spill and a total of 2.7×10^6 events were recorded. The spin direction of the polarized-proton beam was changed every 10 min by 180° using the spin-rotation system. This minimized the systematic errors in the asymmetry measurement. Data were also taken using carbon and copper targets to understand the diffractive background. The data analysis is still in progress, but preliminary results are given here. The average beam polarization is measured as $40 \pm 9 \pm 15\%$, compared to the average tagged-beam polarization value of 45%. The first value of the stated error is statistical, and the second value arises from the uncertainty in the subtraction of the diffractive background process. A small sample of data was taken with the Primakoff-effect polarimeter using polarized incident antiprotons. Even though the amount of data was too small to determine an antiproton-beam polarization, the Primakoff process was clearly observed using antiprotons. Within the systematic and statistical errors discussed above, the Primakoff-effect polarimeter has measured the absolute magnitude and sign of the proton-beam polarization and confirmed the polarization of the beam as measured by the beam-tagging system.

5. Coulomb-Nuclear Interference (CNI) Polarimeter

The CNI polarimeter determines the proton beam polarization by measuring the asymmetry parameter for proton-proton elastic scattering in the Coulomb-nuclear interference region of the momentum transfer squared, $|t| \approx 1$ to $30 \times 10^{-3}\,(\mathrm{GeV/c})^2$. The analyzing power for this process arises from the interference term between the nuclear non-flip amplitude and the electromagnetic spin-flip amplitude,[2] and is approximated by:

$$A(t) = A_m \left(\frac{4z^{3/2}}{3z^2 + 1}\right) . \tag{3}$$

At $z = 1$, $A(t)$ has a maximum value of

$$A_m = \frac{\sqrt{3}}{4}\,(\mu - 1)\,\frac{\sqrt{|t_m|}}{m} , \tag{4}$$

where $z = t/t_m$ and $t_m = 8\pi\alpha\sqrt{3}\,/\sigma_{tot}$. The quantity $(\mu - 1)$ represents the anomalous magnetic moment of the proton, α is the fine structure constant, and σ_{tot} is the total cross section of the reaction. This analyzing power is well-known for both p-p and $\bar{p}$-p interactions, and is virtually independent of the energy. The analyzing power has a maximum value of 4.6% at $t = -3.2 \times 10^{-3}\,(\mathrm{GeV/c})^2$.

The CNI polarimeter, shown schematically in Fig. 8, consists of seven scintillator targets surrounded by lead-scintillator sandwich veto counters, the two sets energy-loss distribution for a minimally-ionizing proton (this requirement does not apply to the stilbene counter), (3) no veto counter signal, (4) a proton scattering angle corresponding to an elastic p-p interaction with $|t| > 0.001\,(\mathrm{GeV/c})^2$, and (5) a calculable proton polarization value from the beam tagging.

Data with the polarized-proton beam were taken during two different periods, accumulating a total of 3×10^6 events in 29 hours. The direction of the vertically-polarized proton beam was periodically reversed by the snake magnets to minimize systematic errors. About 20% of the total number of events had tracks consistent with elastic p-p scattering and $|t| > 0.001\,(\mathrm{GeV/c})^2$; more than one-half of the other events were due to noninteracting protons or very small angle scattering. The measured result is 41 ± 26%, compared to the beam-tagged value of 42%. A small amount of data was taken using the polarized-antiproton beam. Assuming that the analyzing power for inclusive small-angle scattering of antiprotons is the same as that for protons, the measured antiproton beam polarization was 47 ± 16%, compared to an expected value of 43% from the beam-tagging.

The result from the CNI polarimeter, although limited by low statistics, is consistent with the expected average beam polarization as given by the beam tagging system.

6. Large-x_F Pion Production

Along with the measurements made by the two polarimeters, the inclusive production of neutral pions at large x_F has also shown a spin-dependent asymmetry in the production cross section.[3] A nonvanishing analyzing power found in this inclusive reaction means that it can be used as an on-line beam polarization monitor for future experiments. Several features make this an attractive choice: (1) the reaction has a large cross section, (2) detection of the two photons from the π^0 decay is a relatively simple measurement, (3) no charged-particle track reconstruction is necessary, and (4) this detector does not interfere with detectors from other experiments. The required calibration of this polarimeter is provided by the absolute measurements of the Primakoff-effect and CNI polarimeters.

The detector used to measure the position and energy of the two photons is a segmented, electromagnetic calorimeter located 50.5 m downstream of the experimental target. The inner edge of the calorimeter is displaced 30 cm to the right of the nominal beam axis to enhance the acceptance of larger transverse-momentum particles and reduce unwanted backgrounds. The calorimeter consists of two parts: (1) an array of 123 lead-glass blocks, each 6.35 cm × 6.35 cm and of hodoscopes located upstream of the experimental target, a "Gray code" transmission hodoscope,[9] twelve MWPCs, and a dipole analyzing magnet. The trigger for an elastic p-p scattering event is defined by signals from both the scintillating target and the hodoscopes.

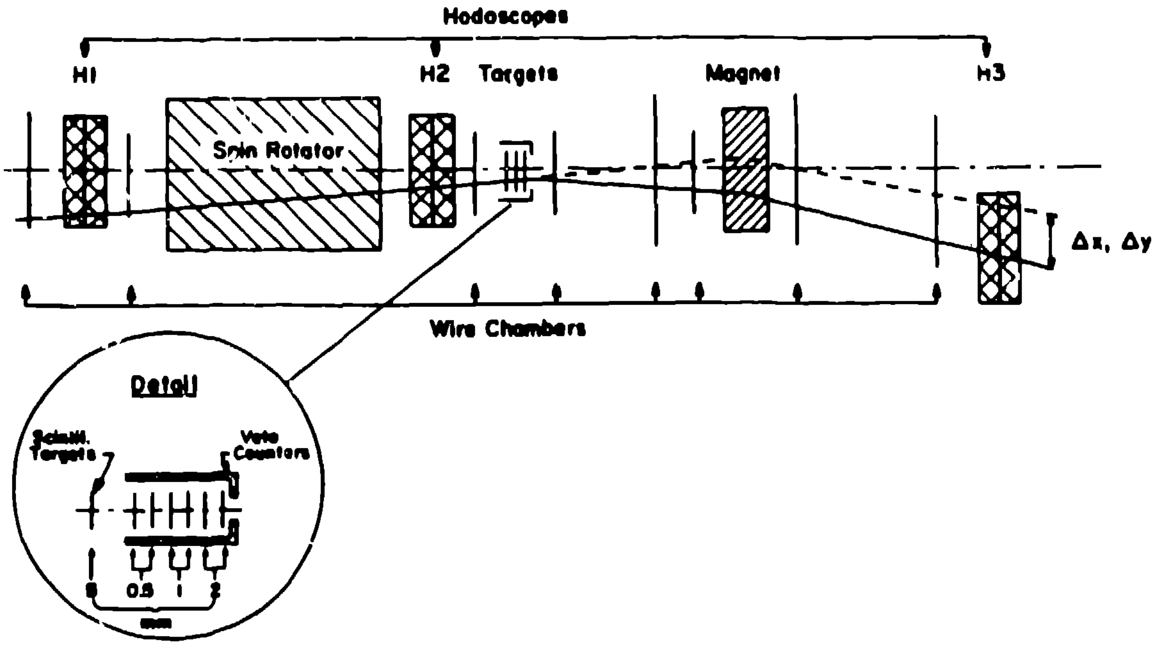

Fig. 8. Layout of the CNI polarimeter. The dimensions transverse to the beam are not to scale.

The target consists of seven scintillation counters, which are 4.0 cm in diameter and range in thickness from 0.5 to 5.0 mm. Six of the scintillation counters are made of Pilot B material and are spaced at 20-cm intervals along the beam direction. The seventh, which is the 5.0-mm counter, is made of stilbene and is located 71 cm upstream of the first plastic scintillator. The signal from each scintillator goes into an ADC so that recoil protons can be separated from the transmitted protons by integrated pulse height. The recoil protons in the region of interest have energies ranging roughly from 1 to 10 MeV, compared to the transmitted protons, which deposit between 0.1 and 0.6 MeV in the plastic scintillators and about 1 MeV in stilbene.

The CNI trigger uses only scintillator information to quickly determine a valid event. The trigger requirements are: (1) only one proton detected before and after the target, (2) at least one signal from the plastic-target scintillators must have a pulse height greater than a threshold that accepts only 5% of the Landau

13 radiation lengths, and (2) a downstream section consisting of a 16-layer, lead-scintillator sandwich calorimeter, with 6.35 mm of lead and 1.27 cm of scintillator per layer. The lead-glass portion absorbs about 75% of the energy in a particle shower and provides the necessary position measurement for the π^0 reconstruction. The blocks are stacked in the shape of a semicircle, placed symmetrically with respect to the horizontal plane, so that the acceptance is the same for pions with the same transverse momentum. The lead-scintillator sandwich portion is divided into five sections vertically, with each section using four photomultiplier tubes. A veto scintillation counter is used upstream of the calorimeter to discriminate charged-particle from neutral-particle events.

A total of 2.85×10^5 triggers were recorded from a total beam flux of 1.17×10^{10} protons. One-half of the data was accumulated with a 10-cm polyethylene target, while the remaining portion used the CNI scintillator target. An average trigger rate was 300 per 20-sec spill, of which 7% reconstructed to a neutral pion. The average beam polarization was 44% for protons with tagged polarization magnitudes between 30 and 55%.

The average analyzing power measured[4] for the inclusive π^0 production at $\langle x_F \rangle = 0.52$ and $\langle p_T \rangle = 0.8$ GeV/c is $10 \pm 3\%$. The analyzing power for background events is consistent with a zero value. With this new analyzing power measurement, the π^0 inclusive process at large x_F can serve as a useful monitor of the beam polarization for future experimental needs.

7. Conclusions

A polarized-proton and polarized-antiproton beam line using a new design has been built and tested at Fermilab. Its successful initial operation at 185 GeV/c makes this the highest-energy polarized-proton beam in the world and the only available polarized-antiproton beam. Future experiments planned for this facility include: a measurement of $\Delta\sigma_L$, the difference in the parallel and antiparallel total cross sections for pure helicity states, the large transverse momentum production of neutral pions and large-x_F production of Λ and Σ° hyperons and pions. Most of the detectors are already set up in the MP-Hall (see Fig. 9) for use in performing these experiments

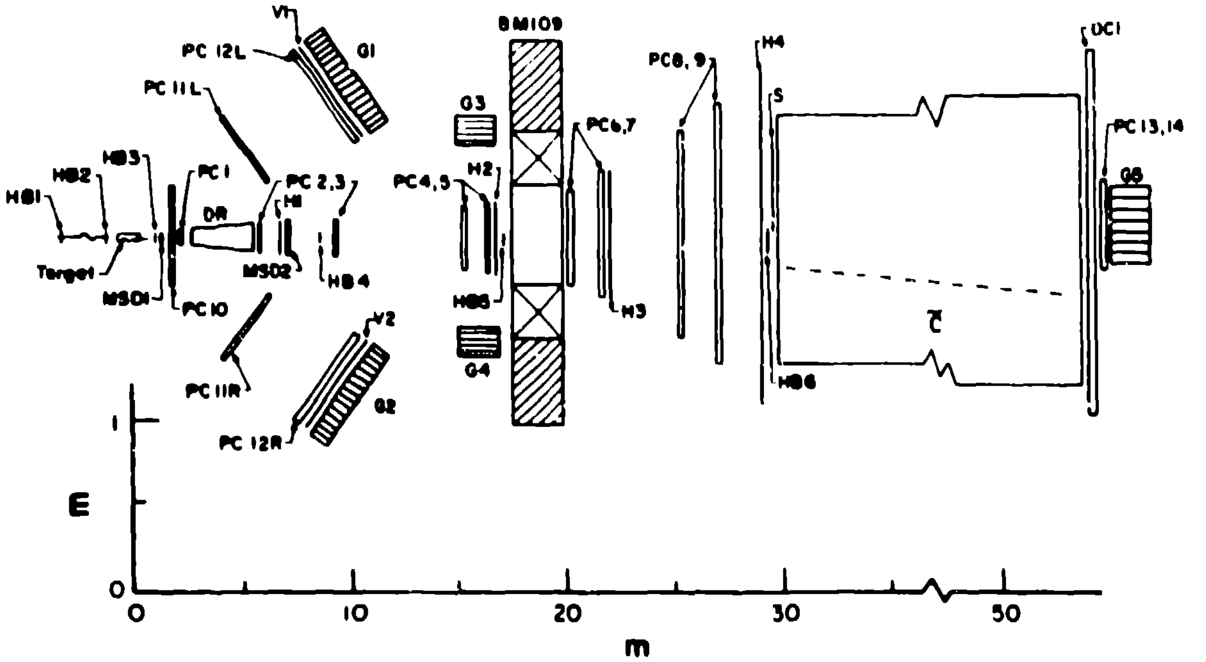

Fig. 9. Detectors in the MP experimental hall (top view) HB1,2,3: beam hodoscope, HB4,5,6: transmission hodoscope, Target: polarized proton/hydrogen target/polarimeter target, H1 to H4: trigger hodoscope, MSD1,2: multistrip detector, PC1 to 14, MWPC, V1,V2: veto hodoscope, G1,2: lead glass calorimter, G3,4: lead glass hodoscope.

8. References

a) Work supported by the United States Department of Energy, Division of High Energy Physics, Contract W-31-109-ENG-38.

b) The E-581/704 Collaboration—N. Akchurin, R. Birsa, F. Bradamante, D. C. Carey, R. N. Coleman, J. D. Cossairt, M. D. Corcoran, A. A. Derevschikov, A. de Lesquen, M. Gazzaly, M. Georgi, D. P. Grosnick, D. A. Hill, K. Imai, K. Kuroda, M. R. Laghai, F. Lehar, D. Lopiano, F. C. Luehring, A Maki, S. Makino, A. Martin, A. Masaike, Yu. A. Matulenko, A. P. Meschanin, A. Michalowicz, D. H. Miller, K. Miyake, T. Nagamine, M. Nessi, F. Nessi-Tedaldi, C. Nguyen, S. B. Nurushev, Y. Ohashi, Y. Onel, G. Pauletta, A. Penzo, G. C. Phillips, A. L. Read, J. B. Roberts, R. A. Rzaev, G. Salvato, R. Schailey, P. Schiavon, G. Shapiro, T. Shima, H. Spinka, V. L. Solovyanov, R. W. Stanek, R. Takashima, F. Takeutchi, N. Tamura, N. Tanaka, S. Dalla Torre-Colautti, D. G. Underwood, L. van Rossum, J. L. White, A. Yokosawa, A. Zanetti.

1] H. Primakoff, Phys. Rev. 81, 899 (1951); A. Halprin, C. M. Andersen, and H. Primakoff, ibid., 152, 1295 (1966); K. Kuroda, AIP Conference Proceedings No. 95, *"High Energy Spin Physics,"*(Brookhaven, 1982), edited by G. M. Bunce (American Institute of Physics, New York 1981), p. 618; D. G. Underwood, Argonne National Laboratory Document ANL-HEP-PR-77-56, 1977.

2] B. Z. Kopeliovich and Lapidus, Yad. Fiz. 19, 218 (1974) [Sov. J. Nucl. Phys. 19, 114 (A74)]; N. H. Buttimore, E. Gotsman, and E. Leader, Phys. Rev. D18, 694 (1978); J. Schwinger, Phys. Rev. 73, 407 (1948).

3] B. E. Bonner et al., Phys. Rev. Lett. 61, 1918 (1988).

4] See for example, *"Proceedings of the Symposium on Future Polarization Physics at Fermilab,"* Fermi National Accelerator Laboratory, Batavia, Illinois, 1988; edited by E. Berger, J. C. Mortin, A. L. Reed, and A. Yokosawa, or *"Proceedings of the VII International Symposium of High Energy Spin Physics,"* Protovino, USSR, 1986 (Serpukhov, 1987).

5] O. E. Overseth, NAL 1969 Summer Study Report, SS-118, Vol. 1.

6] J. W. Cronin and O. E. Overseth, Phys. Rev. 129 (1963) 1795; O. E. Overseth et al., Phys. Rev. Lett. 19 (1967) 391.

7] P. Dalpiaz et al., CERN/ECFA/72/4, Vol. I, p. 284; CERN proposal SPSC, p. 87, July 1977.

8] B. Margolis and G. H. Thomas, in AIP Conference Proceedings No. 42 Higher Energy Polarized Proton Beams, Ann Arbor 1977, edited by A. D. Krisch and A. J. Salthouse (American Institute of Physics, New York, 1978) p. 173; G. Fäldt et al., Nucl Phys. B41, 125 (1972).

9] M. Arignon et al., Nucl. Instrum. & Methods A235, 523 (1985).